ISSN: 2447-3359

REVISTA DE GEOCIÊNCIAS DO NORDESTE

Northeast Geosciences Journal

v. 8, nº 2 (2022)

https://doi.org/10.21680/2447-3359.2022v8n2ID23022

Flooding in accelerated urban expansion scenarios: case study Alto Sumaré neighborhood, Mossoró/RN

Alagamentos em cenários de expansão urbana acelerada: estudo de caso no bairro Alto Sumaré, Mossoró/RN

Tenório José de Brito[1]; Venerando Eustáquio Amaro[2]; Maria de Fátima Alves de Matos[3]

[1] Federal University of Rio Grande do Norte, Department of Civil and Environmental Engineering, Natal/RN, Brazil. Email: tenoriobrito@gmail.com
ORCID: https://orcid.org/0000-0002-6967-9926

[2] Federal University of Rio Grande do Norte, Department of Civil and Environmental Engineering, Natal/RN, Brazil. Email: venerandoamaro@gmail.com
ORCID: https://orcid.org/0000-0001-7357-2200

[3] SENAI Institute for Innovation in Renewable Energy, SENAI-DR-RN, Natal/RN, Brazil. Email: mfatimaalves.m@gmail.com
ORCID: https://orcid.org/0000-0002-2864-2027

Abstract: In the last decade, the Municipality of Mossoró/RN has experienced an accelerated advance in the urban occupation process, promoted in large part by the Minha Casa Minha Vida Program of the Federal Government. Flooding-related problems were reported in the Alto Sumaré neighborhood, treated as the study area. In order to simulate future occurrences of flooding based on the urbanization rate, past occurrences and extreme precipitation events, Geotechnologies were used in the analysis of urban expansion from 2010 to 2019 and mapping of areas susceptible to flooding in the Alto Sumaré neighborhood, associated with the parameters of the drainage system and integrated into a Geographic Information System environment. The results point to an expansion percentage of 180.75% between 2010 and 2017 and 112.75% between 2017 and 2019. This expansion, associated with the installation of an inadequate drainage system, has promoted rapid flow when the volumes of the ponds hit full capacity, which increases the area of contribution and, therefore, the flow downstream, causing overflows and floodings. The accumulation volumes for recurrence times of 5 years presented values greater than the volumes of depressions. The accumulation volumes increase as the recurrence time increases, thus demonstrating that the damping capacity of most lakes is insufficient.

Keywords: Urban expansion; Geoprocessing; Northeast of Brazil.

Resumo: Na última década, o Município de Mossoró/RN tem vivenciado um avanço acelerado no processo de ocupação urbana, fomentado em grande parte pelo Programa Minha Casa Minha Vida do Governo Federal. Foram relatados problemas de alagamentos no bairro Alto Sumaré, tratado como área de estudo. Com objetivo de simular ocorrências futuras de alagamentos baseados na taxa de urbanização, ocorrências passadas e eventos extremos de precipitações, foi empregado o uso de Geotecnologias na análise da expansão urbana no período de 2010 a 2019 e mapeamento das áreas suscetíveis a alagamento do bairro Alto Sumaré, associado aos parâmetros do sistema de drenagem e integrados em ambiente de Sistema de Informações Geográficas. Os resultados apontam um percentual de expansão de 180,75% entre 2010 e 2017 e de 112,75% entre 2017 e 2019. Essa expansão, associada a instalação de um inadequado sistema de drenagem, tem promovido o escoamento rápido quando os volumes das lagoas são atingidos, o que aumenta a área de contribuição e, por conseguinte, o caudal à jusante, causando as inundações e alagamentos. Os volumes de acumulação para tempos de recorrência de 5 anos apresentaram valores maiores que o volumes das depressões. Os volumes de acumulação aumentam a medida em que há um aumento do tempo de recorrência, demostrando assim que a capacidade de amortecimento da maioria das lagoas é insuficiente.

Palavras-chave: Expansão urbana; Geoprocessamento; Nordeste do Brasil.

Received: 14/10/2020; Accepted: 02/08/2022; Published: 09/09/2022.

1. Introduction

Recent studies indicate that the percentage of the world's population exposed to risk of disasters related to bankfull discharge, overflowing and flooding events has increased by 25% since the year 2000 (TELLMAN *et al*. 2021). Likewise, the damage caused by these events has more than doubled over the last 50 years (MUNICH RE, 2005). The distinction between these phenomena is as follows: the transient accumulation of flow in the main channel up to the limit of the water body is defined as bankfull discharge; the natural event triggered by the combination of heavy and rapid rains or long-term rains that cause the channels to spill into the fluvial plain is defined as overflow; and, the accumulation of water on the edges and topographic lows is defined as flooding. Such facts have been recurrent in both urban and rural areas around the world and are challenging for urban planning managers, especially for there being interconnected issues between aspects of the physical environment and the issues inherent to the dynamics of urbanization, which exerts increasing pressure for land for urban expansion (KURZBACH et al., 2013).

The urban population is expected to increase from current 4.4 billion to 6.7 billion in 2050 (ALVES, 2021). This increase will certainly lead to changes in the dynamics of urbanization of the territories and, consequently, in changes in the land use and occupation pattern which will impact the hydrological and hydraulic behavior (MERZ et al., 2010). These results of the effects of accelerated urbanization will be potentially aggravated when combined with the assessments of the impacts of global climate change and its consequences at local scales (AKTER et al. 2018).

Exposure to disasters, as more people are exposed to bankfull discharges, overflowings and floodings, has become one of the main challenges to urban risk management (JHA et al., 2011). This occurs, above all, in cities with disorderly dynamics of urbanization and/or urban planning disjointed from local conditions combined with global climate change, as in the case of the intensification of extreme precipitation events (MARENGO et al., 2013). Bankfull discharges, overflowings and floodings are already the biggest disasters in Europe in economic terms, in terms of property damage, infrastructure, physical injuries and loss of human life, which can directly affect more than half a million people and 40 billion euros in damages per year until 2050 (STERN, 2007; EU-SCIENCE-HUB, 2020).

In Brazil, the Brazilian Atlas of Natural Disasters (CEPED/UFSC, 2013) showed that between 1991 and 2012 there were 31,909 catastrophes, of which 73% were in the last decade alone, most of them related to bankfull discharges, overflowings and floodings. Thus, given the peculiar characteristics that the urban environment brings together, such as the large population density and the resources in material heritage, such events of bankfull discharges, overflowings and floodings in urban areas often gain greater prominence due to the dimension of the damage they cause (FELIZARDO, 2016). Whether the damages are related to the material heritage or to public health, they are often irreparable, as in the case of the loss of human lives.

Urban areas are at greater risk of flooding due to the increased volume of rain runoff and due to greater exposure of people and goods, on account of the resource concentration (SATO, 2006). The complexity of the urban environment and its installed drainage infrastructure have an essential influence on the flow of surface runoff (FELIZARDO, 2016). Most Brazilian cities lack studies dedicated to supporting measures for the prevention and/or mitigation of problems related to rainwater drainage (ANDRADE et al., 2014), since the urban drainage system was built over the years in a discontinuous way and under the aspect of rapid drainage of rainwater (TUCCI, 1995). For this reason, urban planning based on adequate projects must be structured in order to mitigate the harmful effects, given that historical records of bankfull discharges, overflowings and floodings in urban areas demonstrate the inefficiency of the existing drainage system. Therefore, it is important to identify risk indicators that affect the process and variability of urban floods (BANSAL et al., 2015).

Flood management is one of the key steps in mitigating and reducing risk of disasters. Studies have suggested that the identification of risk areas for bankfull discharges, overflowings and floodings, in addition to applying essential risk reduction measures, by structural and/or non-structural means, can effectively reduce damage to an acceptable level, in addition to favoring the understanding of the flood damage at a local scale, for better mitigation and adequate urban management (NAULIN et al., 2013; GUO et al., 2014; DANDAPAT; PANDA, 2017; DAS, 2018; DOU et al., 2018). Hazard analysis and flood risk mapping play a significant role in bankfull discharges, overflowings and floodings, guiding early warning systems, emergency response services, and designing flood risk reduction measures (GUO et al., 2014). ; ZHANG; CHEN, 2019).

To date, several studies have been carried out to assess and map out flood-prone areas in different regions of the world (KIA et al., 2012; TEHRANY et al., 2013; HONG et al., 2018; LIMA et al., 2019). Obtaining adequate data for mapping out bankfull discharges, overflowings and floodings using conventional means and techniques is financially costly, time consuming and sometimes not available at the regional or local hydrographic basin sites, especially in Brazil. For this reason, currently, remote sensing and the Geographic Information System (GIS) offer powerful tools and, in addition to being adequate data sources for managing hazards and susceptibility to bankfull discharges, overflowings and floodings, they also

subsidize the elaboration of predictive scenarios. (ARAÚJO et al., 2018; LIMA et al., 2019). The combination of these tools allows for a more realistic simulation of the characteristics of the watersheds locally, through the elaboration of Digital Elevation Model (DEM) and Digital Surface Models (DSM) that reliably portray the behavior of surface runoff (LIMA et al. 2019).

Therefore, this article aims to analyze the susceptibility of newly established urban residential sectors to rapid flooding events, taking as a case study the Alto Sumaré neighborhood in the southern area of the city of Mossoró, in the State of Rio Grande do Norte (RN). Starting from 2010 and encouraged by the housing policy of the Federal Government known as Programa Minha Casa Minha Vida (PMCMV), an accelerated urban expansion began in Mossoró, in which the Alto Sumaré neighborhood stands out. From the surfacing of the first residential complex, Bella Residence, with 144 houses, new real estate projects were created, such as Cidade Jardim 1 with 568 houses, Residencial Monte Olimpo with 335 houses, and Cidade Jardim 2 with 285 houses, promoting from this period on the rapid impermeabilization of the soil in large areas and the change in drainage conditions of the Apodi-Mossoró river microbasins. The process of urban expansion, through the implementation of these planned residential complexes, brought with it negative aspects, such as the frequent flooding in some recently built areas of the neighborhood (Figure 1). This fact occurred despite the regulations contained in the Master Plan of the Municipality of Mossoró. Hence, such events are indicative that some aspects of the physical environment, such as geomorphological and geological/pedological aspects, may not have been satisfactorily considered in the planning of the drainage system and in the definition of the surface flow that would subsidize the construction of the projects.

Figure 1 – Flooding records in the Alto Sumaré neighborhood: A) Flooding of the streets of Residencial Monte Olimpo on 02/05/2015; B) Flooding of the streets of Residencial Monte Olimpo on 03/01/2017; C) Street flooding in the Alto Sumaré neighborhood on 04/09/2018.
Source: authors (2020).

Thus, this article analyzed the changes promoted in the urban physical environment based on the use of Geotechnologies, such as the Global Navigation Satellite System (GNSS) and remote sensing images, correlated to the parameters of the drainage system and integrated in a GIS environment. In this way, it intends to evaluate flooding events as a basis for the simulation of future events, given the urban urbanization rate known for the neighborhood in the last decade, considering scenarios of extreme precipitation events.

1.1. Study Area Characterization

The Alto Sumaré neighborhood is located on the southern outskirts of the city of Mossoró/RN, in the West Potiguar mesoregion (Figure 2). In the urban mosaic, the Alto Sumaré neighborhood was evaluated as a potential area for urban expansion (PETTA et al., 2009) in an area of 1,196.33 hectares concentrated in subdivisions (SILVA, 2015). It is inserted between the plane coordinates 682,000/67.0008mE and 9,422,500/9,419,000mN of the Universal Transverse Mercator projection system (UTM) Zone 24 South.

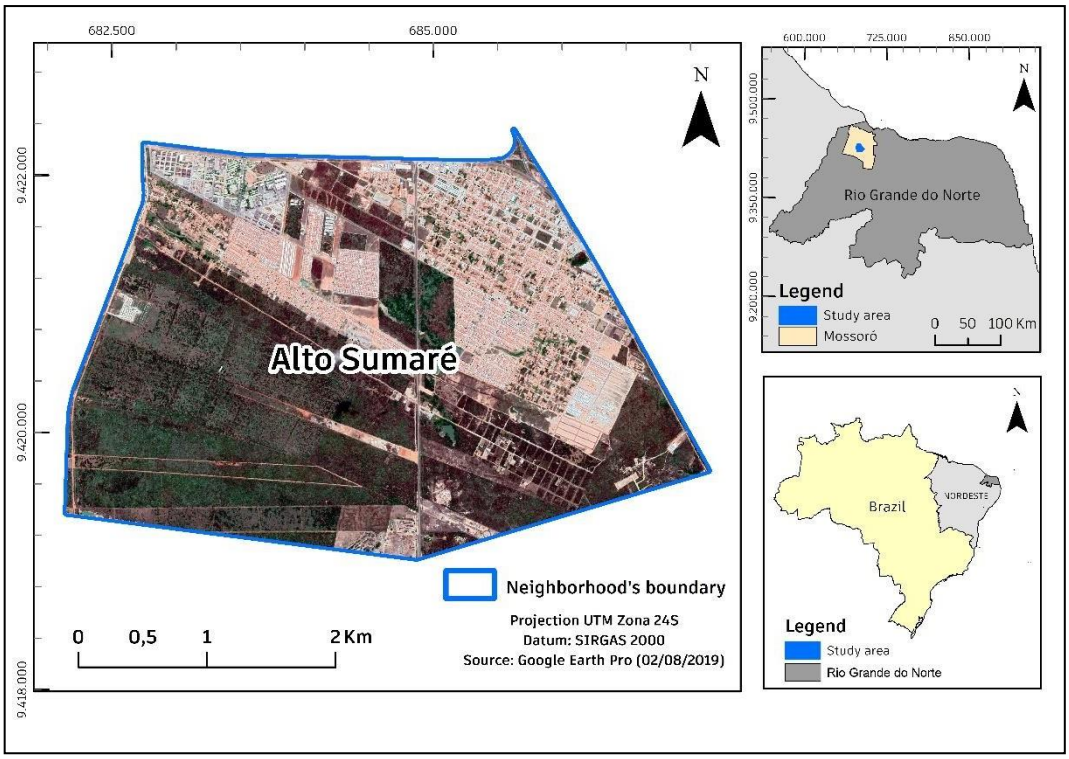

Figure 2 – Location of the study area in the Municipality of Mossoró/RN, Alto Sumaré neighborhood, south of the urban perimeter.
Source: authors (2020).

The Municipality of Mossoró has a hot semi-arid climate of type BSw'h in the Köppen classification, in which the average annual precipitation is 695.8 mm, with an average annual temperature around 27.4°C, with a minimum of 21°C. and a maximum of 36°C (ROCHA, 2015). The relative humidity of air follows the precipitation curve throughout the year, with an observed annual relative average of 68.9%. The dominant winds are from the northeast on 48% of the days, followed by the southeast on 31.50%, which are the most intense (ROCHA, 2015).

In the geological context, the Municipality of Mossoró is located in the central portion of the emerged Potiguar Basin, which is distributed by a larger portion in the RN State and a smaller portion in the western side of the State of Ceará (ARARIPE; FEIJÓ, 1994). In this region, the lithological units belonging to the Jandaíra Formation, the Barreiras Group, the Ancient Alluvial Deposits, the Alluvial Channel Deposits and the Fluvial-Marine Deposits are predominating (CPRM, 2014). Specifically in the study area, the main outcrop lithotypes are from the Jandaíra Formation (98%) composing flat reliefs on the banks and drainage beds, superimposed by the deposits of conglomerates and sandstones of the Barreiras Group, sometimes with clayey matrix and ferruginous concretions, and still covered by gravel and lateritic crusts.

The geomorphology of the region is marked by the relief units of the Coastal Tablelands and the Coastal Plain, with emphasis on Serra do Mel and Serra de Mossoró. The terrain is dissected and shaped by the plain of the Apodi-Mossoró river, which develops as a fluvial-marine plain at the river's mouth on the coastal plain. The relief is flat to slightly corrugated, with low slopes within the order of 0.06° in the northward direction, towards the Coastal Plain. The highest altitudes are

around 250m and are located in the Serra de Mossoró. The study area is part of the Apodi-Mossoró river basin, characterized by flat and low lands where fluvial, transitional or wind accumulation processes occur (CPRM, 2014). In this geographical area, it is subject to intense anthropization, with high levels of land use and occupation, normally disordered, damaging the natural characteristics of the soil and the landscape layout of the entire Apodi-Mossoró River Plain. The soil typologies present in the study area are: Molissols, Vertisols, Litholic Entisol and Red-Yellow Argisols, Litholic Entisol and Quartzarenic Entisols (IDEMA, 2005).

2. Methodology

The methodological procedures which led to the elaboration of maps indicating stretches susceptible to flooding in the Alto Sumaré neighborhood were adapted from the proposals of Abdelsalheen *et al*. (2016) and Lima *et al*. (2019). The steps and activities are described as follows.

2.1. Compilation of historical spatial data and topographic survey

The first stage consisted of a bibliographic research and cartographic surveys of the study area, obtained from public research and public institutions websites. The contour lines were acquired from a partnership with the Engineering Center of the Universidade Federal Rural do Semiárido (UFERSA) and the ENGEFOTO company, which carried out the aerial photogrammetric survey, recruited by PETROBRAS for implementing the no-development zone and areas for complementary installations of the Gas Pipeline from Pilar/AL to Mossoró/RN. The registration of properties and survey of notable points, among others, were also registered. The aerial survey was carried out in 2016 during the rainy season and the contour lines were generated in the Geometric Coordinate System, *datum* SIRGAS2000.

The Ground Control Points (GCP) resulting of the fieldwork were obtained following the methodology suggested by Araújo *et al*. (2018). 23 points were previously defined in the Google Earth Pro application and the location of each GCP was selected in order to achieve the best distribution of planialtimetric positioning in the study area. The need to increase the density of the GCP was identified during the survey, and there were difficulties in accessing some of the previously selected locations (Figure 3).

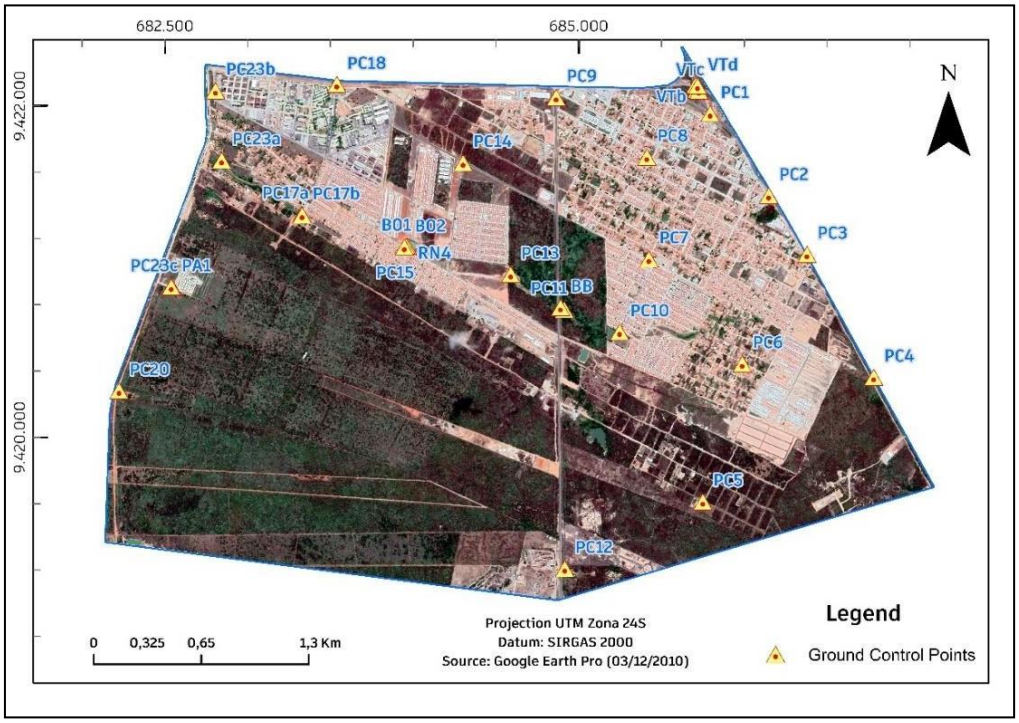

Figure 3 – Distribution grid of ground control points (GCP) in the study area.
Source: authors (2020).

The acquisition was performed using the Real Time Kinematics (RTK) positioning mode, using a dual-frequency L1/L2 receiver, model Kronos 200, with 220 channels and an external radio. Initially, vectors were transported from the point of the Geodesic Station of the Brazilian Geodesic System GPS-92426, with coordinates 9,423,475.572mN-686,363.974mE and geometric altitude of 24,757m, to the base point 001, located on the overpass at the BR-304 highway, within the perimeter of the study area. The collection of 30 total GCP took place on 07/24/2019 (Figure 4).

Figure 4 – GCP collection. A) PC-01, BR-340 highway, Mossoró; B) PC-18, Avenida Wilson Rosado. Source: authors (2020).

2.2. Rainfall data

To evaluate the effects of peak flows on rainfall events and hydrograph generation, the Intensity – Duration – Frequency (IDF) curve proposed by Santos (2015) was used. The parameters for the city of Mossoró were updated through a precipitation series made with data from 1964 to 2013, obtaining the following parameteres: K = 752, 889, a = 0.221, b = 9.778 and c = 0.741, and giving out Equation (1) as output for the rain intensity:

$$I_m = \frac{752{,}889.T^{0{,}221}}{(t+9{,}778)^{0{,}741}} \qquad \text{(Equation 1)}$$

2.3. Data geoprocessing and elaboration of the Digital Elevation Model (DEM)

In this geoprocessing step, the DEM was generated, based on the segmentation of the contours of the topographic survey (Figure 5), using the *Topo to Raster* interpolator (LIMA *et al*., 2016). The DEM highlighted the features of topographic lows, such as the Residencial Bella Residence natural lake, located in the neighborhood, in addition to few elevations and the overpass on the BR-304 highway (Figure 6).

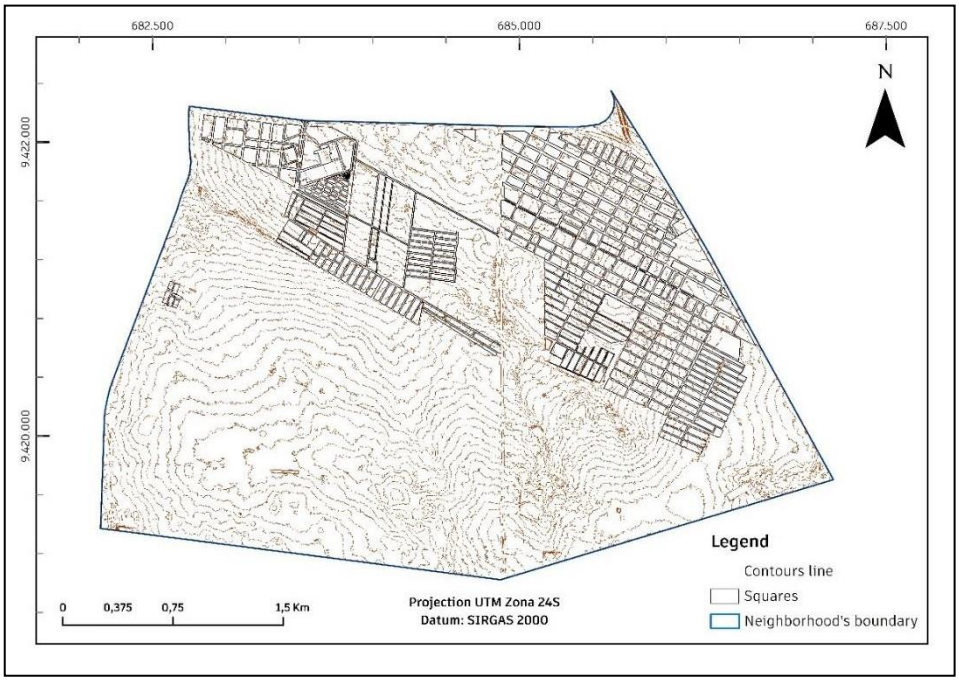

Figure 5 – Segmentation of contour lines for DEM generation and occupied area 2019 of the Alto Sumaré neighborhood, Mossoró/RN.
Source: authors (2020).

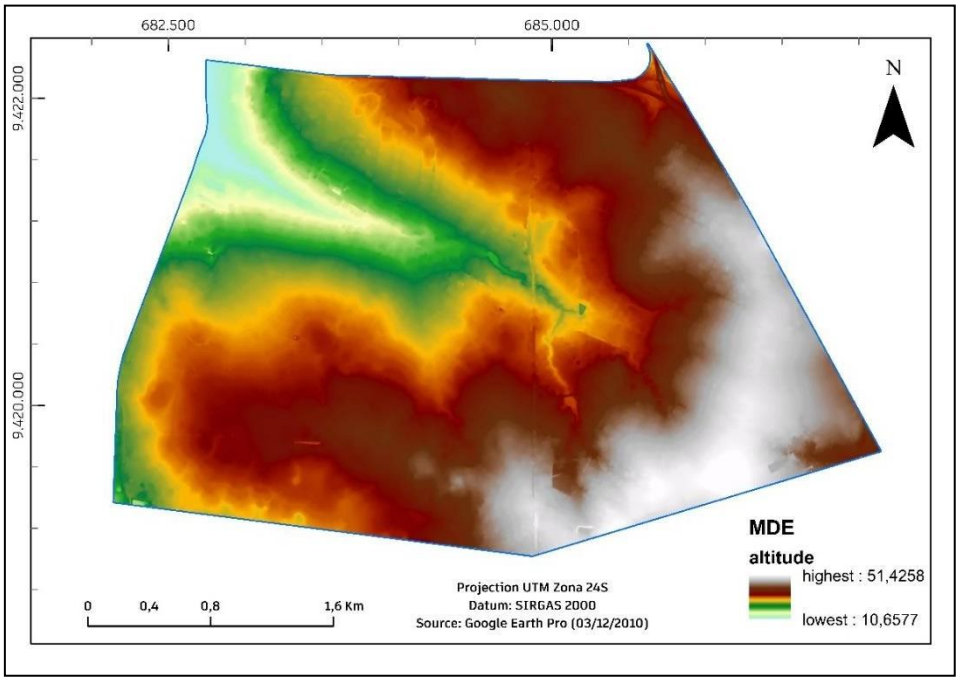

Figure 6 – Digital Elevation Model of the Alto Sumaré neighborhood, Mossoró/RN with altimetric measurement in meters.
Source: authors (2020).

The DEM, when compared to *Google Earth Pro* scenes, showed that transformations were implemented in the watershed after the 2016 aerial survey, with the construction of four retention basins, two in Residencial Cidade Alta, one in Residencial

Campo Belo, and one at the Monte Olimpo Residential. It was thus necessary to update the DEM with the inclusion of these infrastructures (ponds) which directly influence the dynamics of flow and accumulation in the watershed. Hence, concentric polygons were created in the pond areas (Figure 7), adequately spaced so that, when generating the raster model of the ponds, they would present an adequate incline of the pond slope, allowing for the water flow to occur. To each polygon was assigned an altimetric height, zero being assigned to the outermost polygon, and to the inner polygons sequentially decreasing negative values down to the depth of each lake.

The next step was generating the DEM of each pond to add them to the DEM of the study area. Of the four ponds (Residencial Cidade Alta Pond, Residencial Cidade Jardim 1 Pond, Residencial Campo Bello Pond and Residencial Monte Olimpo Pond), only Residencial Cidade Alta Pond was not added to the DEM of the study area, as it is not part of the watershed.

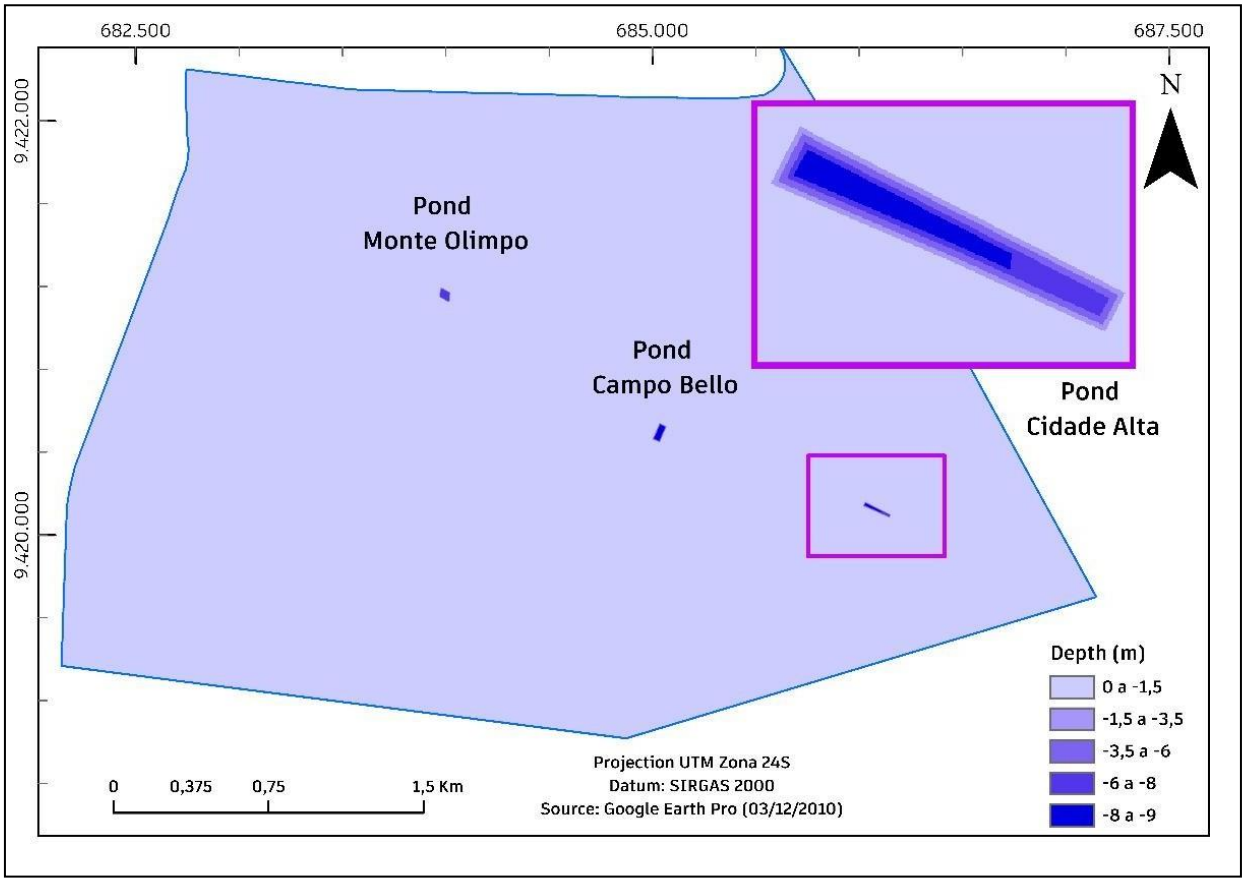

Figure 7 – Digital Elevation Model of the ponds of the Monte Olimpo, Campo Bello and Cidade Alta Residential Houses in the Alto Sumaré neighborhood, Mossoró/RN.
Source: authors (2020).

To correct the 30 GCP, the values of the geoidal ripple (*N*) of the MAPGEO2015 model (IBGE, 2015) were obtained, where corrections for systematic effects were applied, from which the orthometric height (*H*) of each GCP was admitted (Table 1) through the arithmetic calculation: $H = h - N$; where: h = geometric altitude; H = orthometric altitude; N = geoid ripple.

Table 1 – Coordinates and precision of ground control points (GCP).

Name	N Coordinates (m)	E Coordinates (m)	*h* (m)	*N*(m)	*H* (m)
Va	9,422,122.6579	685,705.0029	34.802	-7.22	42.0215
Vb	9,422,093.4660	685,712.5014	34.851	-7.22	42.0712
Vc	9,422,089.2544	685,725.3472	34.705	-7.22	41.9248
Vd	9,422,118.5539	685,717.4446	34.803	-7.22	42.0234
PC1	9,421,951.9033	685,793.9954	29.5934	-7.22	36.8134
PC2	9,421,457.9701	686,146.8043	35.2754	-7.21	42.4854
PC3	9,421,103.6003	686,378.3339	42.666	-7.21	49.8760
PC4	9,420,362.4703	686,781.0706	38.001	-7.20	45.2005
PC6	9,420,443.3702	685,987.8962	35.5880	-7.2	42.7880
PC10	9,420,635.6327	685,246.6401	23.0536	-7.21	30.2636
PC7	9,421,075.1562	685,423.6464	29.7935	-7.21	37.0035
PC8	9,421,689.8325	685,411.4951	33.2245	-7.22	40.4445
PC9	9,422,050.0492	684,863.8691	31.4078	-7.22	38.6278
PC5	9,419,611.9015	685,748.7690	42.0734	-7.19	49.2634
PC12	9,419,208.2793	684,915.1671	42.1574	-7.19	49.3474
PC11	9,420,770.6940	684,912.1105	17.9715	-7.21	25.1815
BB	9,420,782.8014	684,889.7520	18.0321	-7.21	25.2421
PC18	9,422,127.9927	683,538.6006	23.6088	-7.23	30.8388
PC14	9,421,655.8571	684,301.2807	24.6518	-7.22	31.8718
PC13	9,420,982.1447	684,588.6763	15.2726	-7.21	22.4826
PC15	9,421,146.0772	683,964.3480	13.0040	-7.22	20.2240
RN4	9,421,152.0519	683,964.5395	13.607	-7.22	20.8266
PC17	9,421,340.2471	683,328.8795	6.7524	-7.22	13.9724
PC23a	9,421,670.6821	682,843.5783	3.7780	-7.23	11.0080
PC23b	9,422,090.1915	682,806.1587	7.3018	-7.23	14.5318
PC23c	9,420,907.2656	682,542.5277	18.2274	-7.22	25.4474
PA1	9,420,906.7433	682,538.2661	18.328	-7.22	25.5476
B1	9,421,152.1385	683,956.2386	11.683	-7.22	18.9028
B2	9,421,146.5382	683,946.1290	11.700	-7.22	18.9195
PC20	9,420,280.9610	682,223.3760	19.2240	-7.22	26.4440

Where: h = ellipsoidal altitude, N = wave geoid and H = orthometric altitude.

Source: authors (2020).

2.4. Calibration of the DEM and Preparation of the Digital Surface Model – DSM

The DEM calibration was carried out according to the methodology suggested by Araújo et al. (2018). Nine GCP were discarded: PC3 and PC4 for being outside the study area; Vb, Vc and Vd due to their proximity to each other, which could generate a trend during calibration; B1 and B2, collected on the sill of storm drain boxes, as they do not represent the real surface of the land and which, also, could cause an error tendency; RN4, used to change the GNSS antenna, due to proximity to PC15; and PA1, used as a support point for PC23, which presented a higher standard deviation of geometric altitude compared to PC23. Then, the GCP were projected on the DEM *raster* and through the *Extract Values to Points* command in ArcGIS, the altitudes of each GCP were obtained. With the orthometric altitudes of each GCP and the corresponding ones in the DEM, a statistical analysis was carried out (Table 2), where the orthometric altitude value is assumed as a dependent variable [f(x)] and the altitude value in the DEM as an independent variable (x). The comparison of the linear regression equation for 21 GCP and 20 GCP showed that by eliminating the PC17 an improvement in accuracy is obtained with a reduction in the value of the RMSE.

Table 2 – Parameters used in linear regression, H (GCP) – f(x), H (DEM) – x and variations between altimetry (Δ1).

Name	H (GCP)	H (DEM)	Δ1	H (calibrated DEM)
VTa	42.022	41.027	-0.995	41.388
PC1	36.813	36.127	-0.687	36.420
PC2	42.485	42.275	-0.211	42.653
PC6	42.788	42.785	-0.003	43.171
PC10	30.264	29.582	-0.682	29.784
PC7	37.004	36.988	-0.016	37.293
PC8	40.445	40.063	-0.382	40.410
PC9	38.628	38.007	-0.621	38.326
PC5	49.263	49.008	-0.255	49.480
PC12	49.347	49.149	-0.198	49.623
PC11	25.182	24.968	-0.213	25.106
BB	25.242	25.070	-0.172	25.210
PC18	30.839	30.156	-0.682	30.367
PC14	31.872	31.831	-0.041	32.064
PC13	22.483	22.888	0.406	22.998
PC15	20.224	20.002	-0.222	20.071
PC23a	11.008	11.135	0.127	11.081
PC23b	14.532	14.691	0.159	14.686
PC23c	25.447	25.737	0.290	25.886
PC20	26.444	26.159	-0.285	26.314

Source: authors (2020).

In improving the performance of the analysis of surface runoff of rainwater, as described by Lima *et al*. (2019), which highlights anthropic factors in the urban environment, there were used the values applied by Lee *et al*. (2016), who assigned an altimetric value of 0.20m for sidewalks and 20m for urban lots. Values of 0.20m were also adopted for empty lots and 20m for buildings. The values were applied only to buildings because it was verified that, in the surface flow, the rainwater could flow through the lots. These vectors allowed for the generation of the raster, through the *Feature to raster* command, which, added to the calibrated DEM, creates the simplified DSM.

2.5. Surface hydrological modeling

Abdelsalheen et. al (2016) showed that the traditional way of delineating watersheds can be done by using *Arc Hydro tools* from ArcGIS software, which is a systematic process where the effect of storage in depressions is eliminated. This is because the *Fill Sink* tool removes all depressions and produces a hydrologically corrected DEM. Thus, recognizing the areas of rainwater accumulation in urbanized areas is important to correlate with urban elements and evaluate the planning of the watershed.

The identification of depressions in the study area was made using the *Depression Evaluation* tool of the ArcGIS software. In processing, following Lima *et al*. (2019) methodology, topographic lows which depth values were less than 1m, a value defined according to the precision of the data used in the generation of the DEM, were eliminated. The processing generated 31 areas of topographic lows and their respective contribution microbasins.

The volume accumulated in the topographic lows was calculated following the traditional way of delineating hydrographic basins, where the flow direction *raster* was created through the *Flow Direction* command using the simplified DSM. The *raster* with the outflow direction of each cell was then used as the input raster for the *Flow Accumulation* command to generate the flow accumulation.

The identification of the flow lines, generated from the *Stream Definition* command, where the density of the drainage channels was defined, was calculated for areas of influence with a dimension of 7,500 m², due to the extension of the study area and scale used in the analyses. After defining the raster with channel density, they were segmented using the *Stream Segmentation* command for later generation of the layer with the vectors of each channel.

The next step consisted of vectorizing the flow lines through the *Stream to feature* asset of the *Hidrology* set associated with the *Spatial Analyst* feature, of which the input *raster* was the one produced by *Flow Direction* and *Stream Segmentation*. The identification of the longest path within the microbasins of the topographic lows was made through the *Longest Flow Path Catchment* asset, where the *Flow Direction* raster and layer with the areas of contribution of the topographic lows are used as an input parameter. With the generated layer, the initial and final points of the polyline are extracted, which are obtained through the option *Create points on lines*. The last step consists of extracting the altimetric values from the beginning and end of each polyline, which is done using the *Extract value to point* tool. The *Intersect* tool was used to calculate the runoff coefficient of each microbasin, having as input layers the contribution areas of each microbasin and the layer with the urbanized area of the study area.

After identifying the characteristics of each microbasin contributing to the topographic lows, the flow analysis was carried out, according to the method proposed by Abdelsalheen *et al*. (2016), with the characteristics of each microbasin of the topographic lows for the recurrence times, RT = 5, 10 and 25 years (Tables 3).

Table 3 – Characteristics of the contribution area, area of the topographic low, volume of the topographic low and accumulated volume for rainfall with recurrence time, RT = 5, 10 and 25 years.

Depression Contribution (m^2)	**Depression Area (m^2)**	**Depression Volume (m^3)**	**RT = 5 years**		**RT = 10 years**		**RT = 25 years**	
			Vs	**Flood height**	**Vs**	**Flood height**	**Vs**	**Flood height**
112,713.50	22,900.25	23,445.77	873.36	0.04	1,017.94	0.04	1,246.42	0.05
7,310.50	10,257.50	4,230.36	26.71	0.00	31.13	0.00	38.12	0.00
58,405.25	3,877.25	2,306.36	124.63	0.03	145.26	0.04	177.87	0.05
28,881.50	7,577.50	5,552.95	-	0.00	-	0.00	-	0.00
10,036.75	2,402.75	2,637.24	78.24	0.03	91.19	0.04	111.66	0.05
64,613.00	907.50	421.49	155.03	0.17	180.70	0.20	221.26	0.24
18,781.00	1,340.75	394.09	-	0.00	-	0.00	-	0.00
30,317.75	611.75	399.23	4.18	0.01	4.87	0.01	5.96	0.01
3,544.25	2,794.50	15,978.31	-	0.00	-	0.00	-	0.00
8,941.50	567.50	267.12	-	0.00	-	0.00	-	0.00
6,718.75	2,852.00	1,517.57	-	0.00	-	0.00	-	0.00
122,852.75	10,225.00	5,026.59	42.96	0.00	50.07	0.00	61.31	0.01
8,368.50	1,064.50	424.72	11.90	0.01	13.86	0.01	16.98	0.02
187,079.25	28,521.25	49,843.88	203.79	0.01	237.53	0.01	290.84	0.01
19,877.00	3,877.75	6,777.08	84.07	0.02	97.99	0.03	119.98	0.03
482.50	387.25	286.44	-	0.00	-	0.00	-	0.00
78,322.25	2,677.50	1,552.53	2.32	0.00	2.70	0.00	3.31	0.00
18,683.25	4,289.00	4,610.17	2.89	0.00	3.37	0.00	4.13	0.00
4,451.75	2,942.50	13,480.42	2.62	0.00	3.06	0.00	3.75	0.00
44,229.00	1,716.25	1,065.95	0.53	0.00	0.61	0.00	0.75	0.00

Vs – Contribution volume of the topographic low

Source: authors (2020).

The flow lines generated in the previous step were used to calculate the contribution volumes in artificial ponds and other more significant accumulation points. The process consisted of defining the outlet points of each pond and the accumulation point within the flow network, creating a shapefile of points to be used alongside the flow direction raster created with the *Flow Direction* tool as input in the *Watershed* tool in ArcGIS's *Hydrology*. The processing generated a *raster* with the watersheds of each outlet point. The raster file was vectorized using the *Raster to Polygon* asset to calculate the watershed characteristics.

3. Results and discussions

3.1. Calibrated DEM

The calibration performed with 20 GCP by the method proposed by Araújo et al. (2018) proved itself to be robust, presenting the parameters $R^2 = 0.999$ and $p < 0.001$ (Figure 8), from which it can be concluded that there is a strong correlation between the control points collected through GNSS and the DEM. The model provided the regression equation: y = 1.0139 x - 0.2087, which was used in the calibration of the DEM, in which the altimetry value of each pixel of the DEM represented the value of x, returning the altimetric value y of the calibrated DEM.

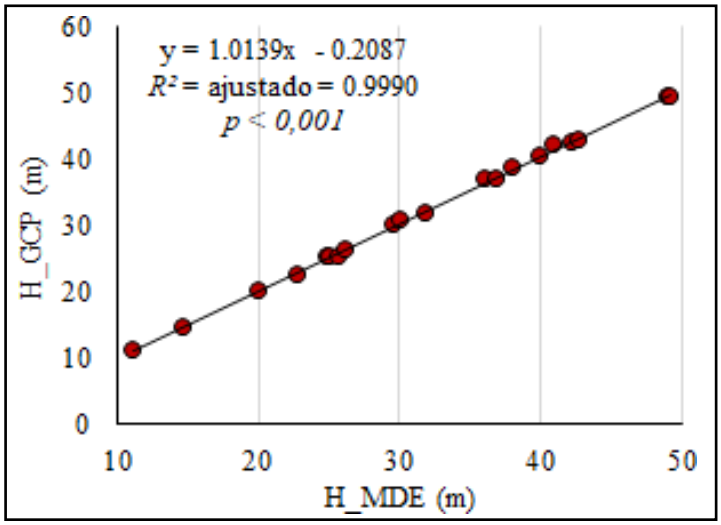

Figure 8 – Comparison H_GCP (Bases of Reference) and H_DEM by Linear Regression.
Source: authors (2020).

In the descriptive statistics of the data it stands out, based on the average variation of the height of the control points in relation to the height of the uncalibrated DEM, with a value of -0.234m, that the plane of the uncalibrated DEM was above the level of the control points (Table 4). The average variation of the control points and calibrated DEM presented zero value, due to the adjustment of the DEM plane to the plane of control points.

There was also a simple reduction in the RMSE parameter of the uncalibrated DEM (22.50%), with a value from 0.40 to 0.31 of the calibrated DEM. This is due to the fact that the topographic database used in the generation of the DEM was produced by laser profiling following the 2016 aerial survey.

Table 4 – Descriptive statistics of altimetric data for the study area.

	H - GCP (m)	**H - DEM (m)**	**ΔH = H (GCP) - H (DEM)**	**H – calibrated DEM**	**ΔH = H (GCP) - H (calibrated DEM)**
Minimum	11.008	11.135	-0.995	11.081	-0.633
Median	31.355	30.994	-0.212	31.215	0.020
Average	32.117	31.882	-0.234	32.117	0.000
Maximum	49.347	49.149	0.406	49.623	0.515
Std. error	2.425	2.390	0.081	2.424	0.074
Variance	117.594	114.289	0.130	117.486	0.108
Std. deviation	10.844	10.691	0.361	10.839	0.329
RMSE (m)		**0.40**		**0.31**	

Vs – Contribution volume of the topographic low for a RT = 25 years
Source: authors (2020).

3.2. Process of urban occupation in the study area

In 2000, the resident population in the Alto do Sumaré neighborhood was 3,947 inhabitants, while in the following decade this number grew by 64.25% (Table 5). Such growth was greater than the total population growth of Mossoró, a population increase that already showed the potential of the study area for urban expansion.

Table 5 – Population growth in the study area from 2000 to 2010.

Population			Percentual growth
Location	**2000**	**2010**	
Alto do Sumaré	3,947	6,483	64.25%
Mossoró	213,841	262,076	22.56%

Source: CENSO 2000, CENSO 2010, IBGE.

The occupation in the neighborhood started in both the northeast and part of the northwest portions, where the presence of the PETROBRAS UN-RNCE/ATP-MO unit stands out, which represented 5.62% of the total area of the neighborhood (Table 6). As of 2010, the second phase of occupation took place in the Alto Sumaré neighborhood, with growth vectors from the northeast portion towards the southern part of the neighborhood, as well as towards the central-west part (Figure 9).

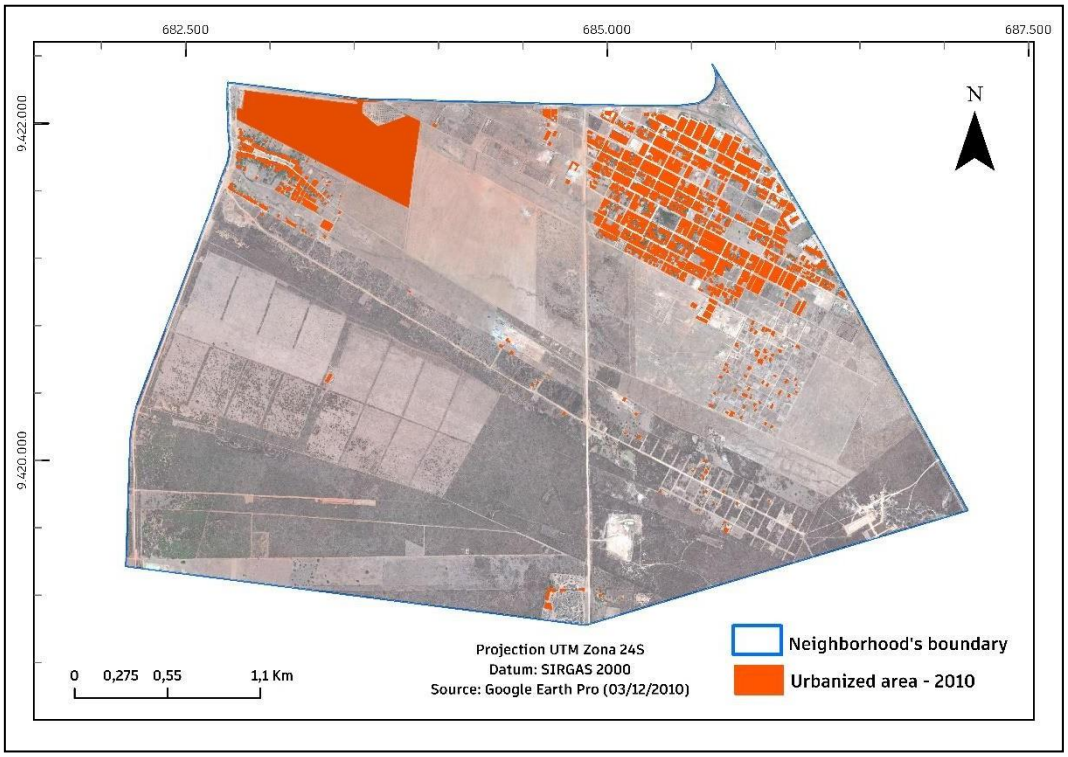

Figure 9 – Urban occupation of the Alto do Sumaré neighborhood in 2010.
Source: authors (2020).

In 2017, the percentage of occupied area in the neighborhood was 10.15%, which represents an 80.75% growth rate of occupancy in the neighborhood. The urban expansion of the northeast portion had already been consolidated with the construction of the Bella Residence and Cidade Jardim 1 residential enterprise, and the occupation of the central-west portion of the neighborhood started with the construction of the Monte Olimpo, Cidade Jardim 3 and Bosque dos Pássaros residential enterprise. (Figure 10).

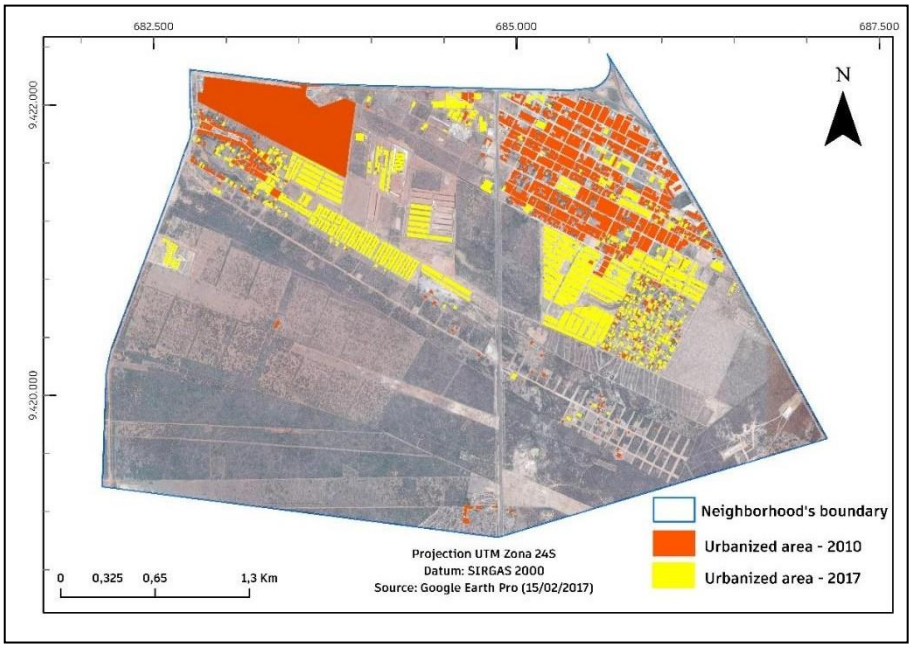

Figure 10 – Urban occupation of the Alto do Sumaré neighborhood in 2017.
Source: authors (2020).

In 2019, the expansion of the southeastern part of the Alto do Sumaré neighborhood began with the construction of the Cidade Alta and Campo Bello residential enterprise, in the central-west portion there was also the completion of the residential Bosque dos Pássaros and Village do Oeste (Figure 11). In the 2017 – 2019 biennium, the expansion rate in the neighborhood was expressive, around 12.75% (Table 6).

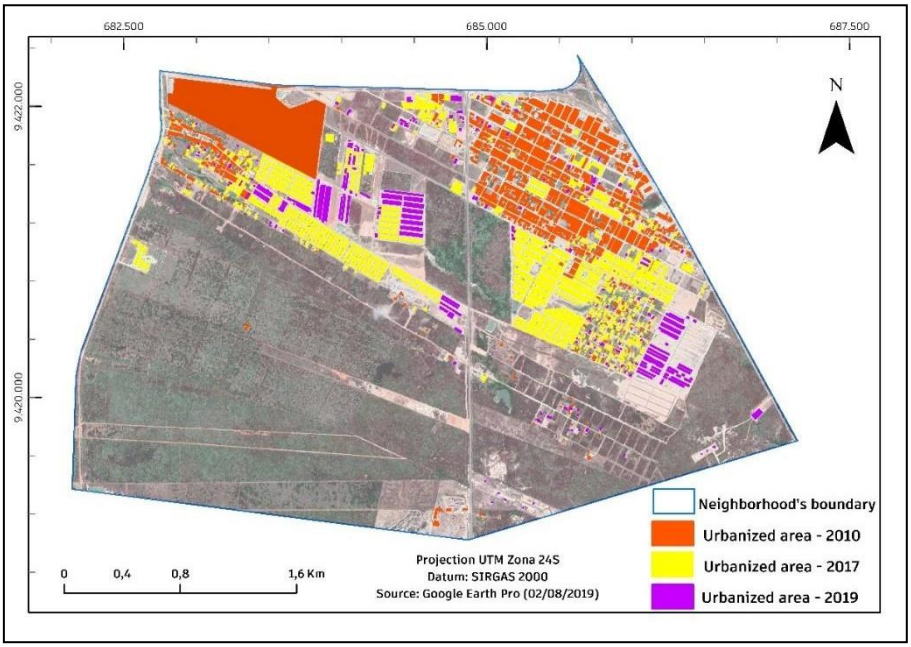

Figure 11 – Urban occupation of the Alto do Sumaré neighborhood in 2019.
Source: authors (2020).

Table 6 – Growth of the occupancy area in the study area from 2010 to 2019. Area of the neighborhood: 11,963,277.05 m².

Year	Total constructed area	Occupation rate	Population growth rate
2010	671.807,17	5,62%	-
2017	1.214.265,28	10,15%	80,75%
2019	1.369.084,55	11,44%	12,75%

Source: CENSO 2000, CENSO 2010, IBGE.

3.3. Simplified Digital Surface Model (DSM)

The simplified DSM incorporated anthropic features to the DEM, which are essential elements in the flow lines analysis. In the shaded map on Figure 12 it can be seen, by associating the history of urban expansion of the Alto Sumaré neighborhood described above, that urban growth has increasingly occupied low-relief sectors, which are the most prone to flooding.

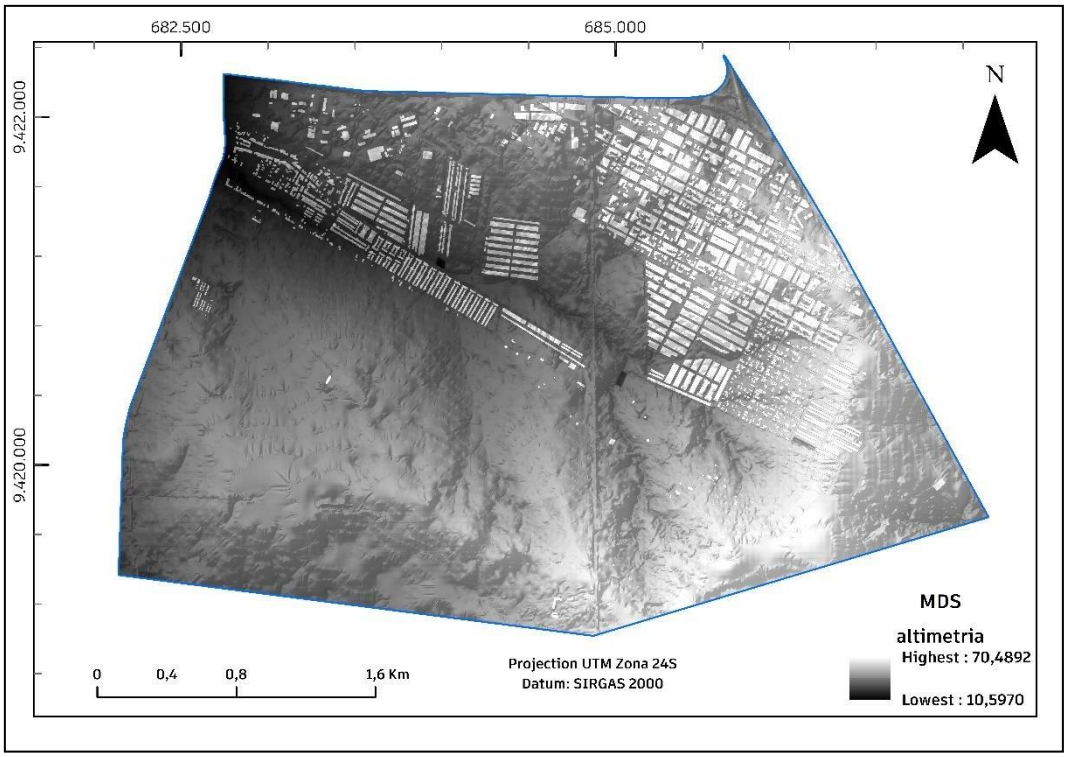

Figure 12 – Simplified Digital Surface Model of the Alto do Sumaré neighborhood
Source: authors (2020).

3.4. Topographic depressions and flow network

Applying the *Depression Evaluation* processing routine on the DSM resulted in the identification of depressions or topographic lows and their respective areas of contribution. The resulting product exhibited all topographic lows where surrounding cells converge to a cell of lower altimetry. Thus, the generated map also showed areas which depressions were less than 1m deep. However, the simplified DSM originated from metric precision contour data and, therefore, topographic lows with a depth of less than 1m were discarded, leaving 31 significant topographic lows (Figure 13).

Topographic lows 530937, 527996, 521741 and 518329 were already expected, as they are artificial ponds (Residential ponds: Cidade Alta, Cidade Jardim, Monte Belo and Bosque dos Pássaros 1 respectively); Likewise, the topographic lows 530741, 531038, 531356, 531637, 531315, 531270, 514668 are small dams built along the main thalweg, in addition to the topographic lows 527748, an area upstream of the culvert on the BR-110 highway associated with the artificial lake, and 523792 , the area bordering the residential Bosque dos Pássaros 2, which periodically floods.

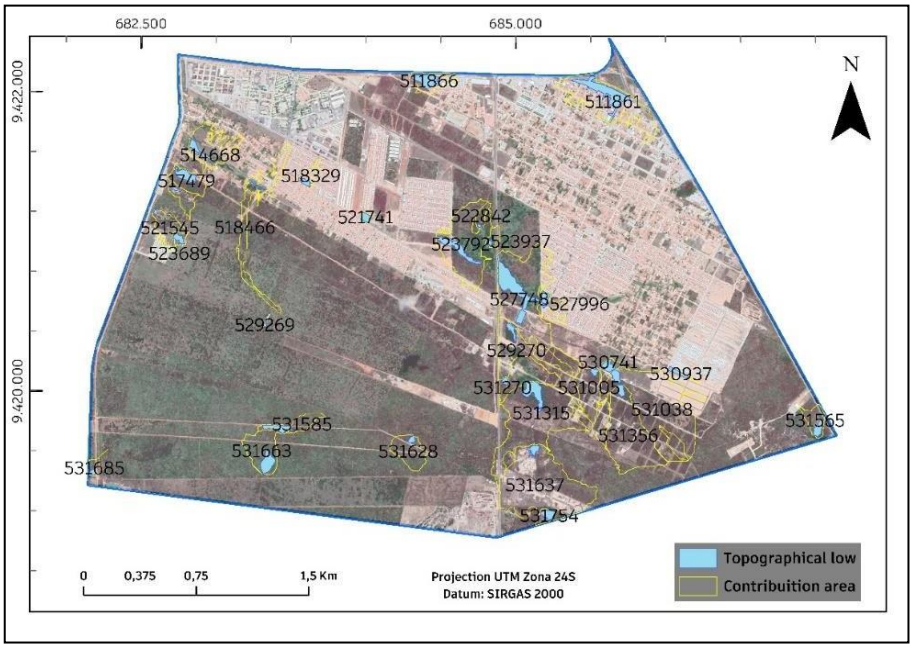

Figure 13 – Topographic depressions in the Alto do Sumaré neighborhood.
Source: authors (2020).

The flow networks represented the expected result, both for the urbanized area and for areas not yet occupied and/or natural, demarcating the surface runoff (Figure 14). The design in the urbanized area occurred predominantly through the street pattern, which demonstrates one of the main effects of human action in urbanization, with earthworks and street paving, in exercising a preferential path for the flow lines. Also, the free area of urban occupation presented flow lines at the lowest points, where the preferential paths of surface runoff are formed.

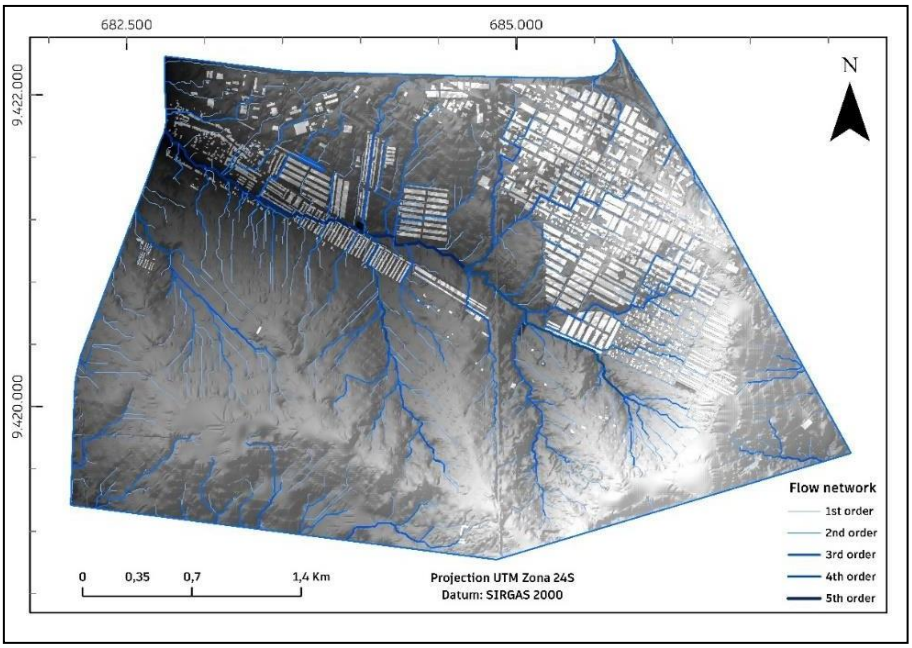

Figure 14 – Flow network in the Alto do Sumaré neighborhood.
Source: authors (2020).

3.5. Contribution volumes in constructed artificial basins

The urbanization process, when it precedes residential developments, imposes the interconnections of flow networks on land use and occupation. Such interconnections occur both by altering the natural relief, which is checked by the earthworks on large areas for real estate purposes, where the layout of the streets create a flow conditioned to the runoff, and by the interconnection of the microbasins through hydraulic works, such as galleries and channels. Thus, the adopted surface runoff model available in the ArcGIS software acts by eliminating the depressions and peaks of the DEM to form a continuous drainage system.

The definition of the outlet points upstream of the artificial lakes of the topographical depressions and the flow network allowed for the delimitation of the contribution area of the microbasins of each lake, as well as allowed finding out the characteristics of the microbasins, such as: most extreme point, altimetric height of beginning and end and the urbanization pattern of each basin. With these characteristics, the calculations of the accumulation volumes of each microbasin were carried out for the RT of 5, 10 and 25 years (Table 7), considering the urbanization of the entire contribution area.

Table 7 – Characteristics of the contribution area, area of the topographic low, volume of the topographic low and accumulated volume for a rainfall with recurrence time, RT = 5 years, RT = 10 years and RT = 25 years.

Contribution Depression (m^2)	Urbanized Area (m^2)	Vol, Depressions (m^3)	Vs (m^3) RT = 5 years	Vs (m^3) RT = 10 years	Vs (m^3) RT = 25 years	Cushioning pond
260,133.44	260,133.44	23,445.77	4,411.03	5,141.23	6,295.23	Overpass at BR-304 highway
24,349.77	24,349.77	2,637.24	553.66	645.32	790.17	R. Bosque dos Pássaros 1 Pond
8,919.86	8,919.86		-	-	-	
40,409.03	40,409.03		-	-	-	
585,153.08	585,153.08	2,306.36	11,609.81	13,531.71	16,569.04	Downstream end dam
980,689.51	980,689.51	421.49	21,249.54	24,767.21	30,326.47	Monte Olimpo final manhole
4,452.27	4,452.27	13,480.42	136.41	159.00	194.68	R. Cidade Alta Pond
855,058.66	855,058.66	6,777.08	21,488.11	25,045.27	30,666.95	Cidade Jardim 1 Pond
8,100.53	8,100.53		-	-	-	
18,853.08	18,853.08	4,610.17	465.09	542.09	663.76	Dam of R. Campo Bello
788,194.80	788,194.80		16,107.93	18,774.46	22,988.58	
560,270.72	560,270.72	49,843.88	14,501.37	16,901.94	20,695.76	Upstream pond manhole BR-110
257,425.33	257,425.33	2,366.07	7,114.53	8,292.28	10,153.57	Dam área R. Campo Bello
1,345,327.43	1,345,327.43	5,026.59	35,046.16	40,847.74	50,016.44	Natural lake close to B. Pássaros 2
131,683.24	131,683.24	3,373.99	3,688.09	4,298.62	5,263.49	Dam área R. Campo Bello
23,605.00	23,605.00		-	-	-	
337,788.66	337,788.66	14,611.36	9,180.50	10,700.25	13,102.04	Upstrem natural lake
2,047,111.94	2,047,111.94	15,978.31	49,597.94	57, 808.44	70,784.15	R. Monte Olimpo Pond
213,737.96	213,737.96		6,085.09	7,092.42	8,684.39	

Source: authors (2020).

The accumulated volumes calculated for a rainfall with TR of 5 years presented values greater than the volume of the depression, that is, the volumes calculated in the Cidade Jardim 1 and Residencial Monte Olimpo ponds, with 21,488.11 m^3 > 6,777.08 m^3 and 49,597, 94 m^3 > 15,978.31 m^3, respectively. In addition, two of the small dams present where the Residencial Campo Bello project was installed also had an accumulated volume greater than the volume of the depression calculated in the simplified DSM. Another point that showed a damping capacity by the depression lower than the accumulated volume for the 5-year TR was the existing natural lake near Bosque dos Pássaros 2, with an accumulated volume of 35,046.16 m^3, greater than the volume of the depression of 5,026.59 m^3.

The culvert at the downstream end of the flow line (main thalweg), the final portion of the Monte Olimpo Residential by topographic low 515466, presented an accumulated volume of 21,249.54 m³ greater than the volume of the depression, which is 421.49 m³. The dam's damping capacity at the downstream end of the study area also presented an accumulated volume of 11,609.81 m³, greater than the dam's damping capacity which has a volume of 2,306.36 m³ calculated through the simplified DSM. Accumulation volumes increase as the recurrence time (TR) increases.

The study did not address the dynamic aspect of the functioning of the damping devices in the hydrographic basin. However, it is observed that most of the surface runoff buffers existing in the study area have limited operation, as both small dams and artificial ponds, such as the Cidade Jardim 1 and Residencial Campo Bello ponds, do not have a bottom spillway. The existence of this type of device is indispensable in open hydrographic basins, in order to allow for the ponds to function as a buffer, since as rains occur, the pond buffers the discharge peak, allowing lower flows downstream, compatible with pre-urbanization flows, thus avoiding higher discharges downstream. When there is no bottom spillway, the ponds only allow for a temporary damping to take place until the complete filling and consequent overtopping of the overflow weir. Such situations can generate a false sense of security, because in periods of higher rainfall, when rain events occur continuously, not allowing adequate time for infiltration and evaporation of the accumulated volume, rains with short recurrence times are sufficient so that the entire upstream area contributes with large downstream discharges, thus generating an increase in surface runoff and overflowing and flooding of the downstream lands.

4. Conclusion

In this article, aspects related to urban growth and flooding were addressed. The study evaluated the planned urban growth of the Alto Sumaré neighborhood in Mossoró/RN. In the urban occupation process, the installation of housing developments predominated, where several residential complexes were built. The area is predominantly flat and had the highest growth between the years 2017 to 2019, with a growth rate of 12.75% occupancy in the neighborhood.

The installed projects occupied both the highest parts of the relief and also the low areas, where the main flow line of the hydrographic microbasin is concentrated. The infrastructure of the drainage systems presents aspects of flow due to incomplete damping, given that most ponds and small dams are installed under the concept of piled accumulation, with no constant and gradual emptying device.

The use of geotechnologies applied to the analysis of areas susceptible to flooding proved to be adequate in this case study, as it allowed for the identification of areas most favorable to the formation of floodable points, which should have restrictions on their use for real estate purposes. The adaptation of the methodology review approach proposed by Abdelsalheen *et al*. (2016) did not show significant adherence to the study area, as the calculated accumulation volumes, taking the contribution area of the topographic lows, did not show a significant approximation to the volume of depressions, even for rains with a recurrence time of 25 years. More investigations should be carried out to understand and better parameterize the process. The evaluation of larger areas of contribution, which form the sub-basins of the areas of contribution of the lakes and significant topographic lows of the study area, showed accumulation volumes that deserve to be highlighted when it comes to alerting the residents of the areas of influence. In this case, it is understood that more detailed studies, where the dynamic aspects of the interrelationship of the damping of ponds and small dams are evaluated, should be carried out for a better delineation of the risks of floodings and overflows. However, the absence of an integrated analysis of the macrodrainage planning showed that the system poses a risk to residents. In 2017, during the implementation of the Monte Olimpo Residential Damping Lake, the occurrence of some precipitation events already caused floodings and overflows in the Monte Olimpo residential.

In fact, the results showed the effect of urbanization and urban expansion that, when added to the impacts of climate change, especially extreme precipitation events, suggest to managers of urban spatial planning and emergency planning the risks they pose to the population.

Therefore, the detailing of the quantification of the elements of the physical environment and of extreme precipitation events are equally relevant in the prediction and management of risks for overflows and urban flooding. In predictive terms, they are considered even more complex, compared to merely river floods, as they require accurate measurement and forecasting of local rainfall in short periods of time. Thus, the elaboration of more detailed models, based on continuous and uninterrupted series of data, are fundamental in the evaluation of the effects of flooding in urban areas, where rivers and urban drainage strongly interact. The flow forecast for a series of precipitation intensities at different recurrence times is fundamental in the management of the risk of bankfull discharges, overflowings and floodings, as a guide for adaptation strategies related to the prediction of bankfull discharges, overflowings and floodings, in a way that avoids underestimating the peak runoff in areas that are already urbanized and on land where expansion of urbanization is planned.

Therefore, it is recommended for future studies to evaluate the impact on the fluvial dynamics of the Mossoró River, as the study area is upstream of the river, which allows for the association of an increase in the contribution of surface runoff with the direct influence of risks in the central areas of the city of Mossoró, installed downstream of the contribution area of the Alto Sumaré neighborhood.

Acknowlegdements

The authors thank the Graduate Program in Civil and Environmental Engineering at UFRN, the Laboratory of Applied Geotechnologies, Coastal and Oceanic Modeling at the Department of Civil and Environmental Engineering at UFRN, Prof. Dr. Paulo Victor do Nascimento Araújo, MSc. Caio Cortez de Lima, Profa. Dra. Ada Cristina Scudelari and Eduardo Baptista Guadain for their support.

References

ABDELSALHEEN, M.; ELMOUSTAFA, A.; HASSAN, A. Evaluation of Depression Storage Using Grid-Based GIS Model. *International Journal of Science and Research*, v. 7, n. 9, 285-289, 2018.

AKTER, T.; QUEVAUVILLER, PH.; EISENREICH, S.; VAES, G. Impacts of climate and land use changes on flood risk management for the Schijn River, Belgium. Environmental Science & Policy. 89. 2018. 10.1016/j.envsci.2018.07.002.

ALVARES, C.A.; STAPE, J.L.; SENTELHAS, P.C.; GONÇALVES, J.L.M.; SPAROVEK, G. Köppen's climate classification map for Brazil. *Meteorologische Zeitschrift*, v. 22, n. 6, 711-728, 2013.

ALVES, J. E. D., O mundo mais urbanizado e as cidades virando saunas. Disponível em: https://www.ecodebate.com.br/2021/01/27/o-mundo-mais-urbanizado-e-as-cidades-virando-saunas/. Acesso em 05/04/2022.

ANDRADE, S. L.; FERREIRA, V. O.; SILVA, M. M. Elaboração de um mapa de risco de inundações da bacia hidrográfica do córrego São Pedro, área urbana de Uberlândia-MG. *Caderno de Geografia*, v. 24, n. 41, p.1–16, 2014.

ARARIPE, P.T.; FEIJÓ, F.J. Bacia Potiguar. *Boletim de Geociências da Petrobrás*, v. 8, n. 1, 127–141, 1994.

ARAÚJO, P.V.N.; AMARO, V.E.; ALCOFORADO, A.V.C.; SANTOS, A.L.S. Acurácia vertical e calibração de modelos digitais de elevação (MDEs) para a Bacia Hidrográfica Piranhas-Açú, Rio Grande do Norte, Brasil. *Anuário do Instituto de Geociências*, v. 41, n. 1, 351-364, 2018.

BANSAL, N.; MUKHERJEE, M.; GAIROLA, A. Causes and impacto of urban flooding in Dehradun. *International Journal of Current Research*, v. 7, n. 2, 12615-12627, 2015.

CEPED/UFSC. Atlas Brasileiro de Desastres Naturais, 2ª edição, Florianópolis, CEPED/UFSC, 2013.

CPRM. Companhia de Pesquisa de Recursos Mineral. Geologia e recursos minerais da Folha Mossoró, estado do Rio Grande do Norte: texto explicativo. Organizadores: Sérgio Willian de Oliveira Rodrigues, Vladimir Cruz de Medeiros Brito. Recife, PE: CPRM, 72p. 2014.

DANDAPAT, K.; PANDA, G.K. Flood vulnerability analysis and risk assessment using analytical hierarchy process. *Model Earth Syst Environ*, v. 3, 1627–1646, 2017.

DAS S. Geographic information system and AHP-based flood hazard zonation of Vaitarna basin, Maharashtra, India. Arab. *Journal of Geosciences*, 11, 2018.

DOU, X.; SONG, J.; WANG, L.; TANG, B.; XU, S.; KONG, F.; et al. Flood risk assessment and mapping based on a modified multi-parameter flood hazard index model in the Guanzhong Urban Area, China. *Stoch Environ Res Risk Assess*, v. 32, 1131–1146, 2018.

FELIZARDO, L. M. Aplicação de Sistema de Informações Geográficas (SIG) para modelagem de eventos críticos de vazão em uma microbacia. 2016. 98f. Dissertação (Mestrado em Recursos Hídricos e Tecnologia Ambiental). Programa de Pós-Graduação em Recursos Hídricos e Tecnologia Ambiental, Universidade Estadual Paulista, Ilha Solteira-SP, 2016

GUO E, ZHANG J, REN X, ZHANG Q, SUN Z. Integrated risk assessment of flood disaster based on improved set pair analysis and the variable fuzzy set theory in central Liaoning Province, China. *Natural Hazards*, v. 74, 947-965, 2014.

HONG, H.; PANAHI, M.; SHIRZADI, A.; MA, T.; LIU, J.; ZHU, A.X. et al. Flood susceptibility assessment in Hengfeng area coupling adaptive neuro-fuzzy inference system with genetic algorithm and differential evolution. *Science of Total Environment*, v. 621, 1124–1141, 2018.

INSTITUTO BRASILEIRO DE GEOGRAFIA E ESTATÍSTICA - IBGE, 2001.Resultados da Amostra do Censo Demográfico 2000 - Malha municipal digital do Brasil: situação em 2001. Rio de Janeiro: IBGE, 2004. Fonte: IBGE, Resultados da Amostra do Censo Demográfico 2000 NOTA: Informações de acordo com a Divisão Territorial vigente em 01.01.2001. 2001

IBGE – INSTITUTO BRASILEIRO DE GEOGRAFIA E ESTATÍSTICA. Censo Brasileiro de 2010. Rio de Janeiro: IBGE, 2012.

INSTITUTO DE DESENVOLVIMENTO ECONÔMICO E MEIO AMBIENTE DO ESTADO DO RIO GRANDE DO NORTE. Atlas para a promoção do investimento sustentável no Rio Grande do Norte. módulo I: zona homogênea mossoroense. Natal: IDEMA, 2005. 205 p. 1 atlas

JHA, A.; LAMOND, J.; BLOCH, R.; *et al*. Five Feet High and Rising – Cities and Flooding in the 21st Century, Policy Research Working Paper 5648. The World Bank, Washington, 2011.

KIA, M.B.; PIRASTEH, S.; PRADHAN, B.; MAHMUD, A.R.; SULAIMAN, W.N;A; MORADI, A. An artificial neural network model for flood simulation using GIS: Johor River Basin, Malaysia. *Environment Earth Science*, v. 67, 251-264, 2012.

KURZBACH, S.; HAMMOND, M.; MARK, O.; SLOBODAN DJORDJEVIC, S.; et al. The development of socio-economic scenarios for urban flood risk management. NOVATECH, 1-10, 2013.

LEE, S.; NAKAGAWA, H.; KAWAIKE, K.; ZHANG, H. Urban inundation simulation considering road network and building configurations. *Flood Risk Management*, v. 9, 224-233, 2016.

LIMA, C.C.; AMARO, V.E.; ARAÚJO, P.V.N.; SANTOS, A.L.S. Identificação e avaliação de zonas de alagamentos urbanos, com suporte de geotecnologias, na cidade de Natal, Nordeste do Brasil. *Anuário do Instituto de Geociências*, v. 42, n. 2, 378-394, 2019

LIMA, F.G.F.; AMARO, V.E.; SANTOS, M.S.T.; SANTOS, A.L.S. Avaliação de métodos de interpolação na geração de modelos digitais de elevação de precisão em zonas costeiras de alta dinâmica sedimentar. *Revista Brasileira de Cartografia*, v. 68, n. 3, 527-538, 2016.

MARENGO, J.; RAMÍREZ, V.; OBREGÓN, G. Observed and projected changes in rainfall extremes in the Metropolitan Area of São Paulo. *Climate Research* 57. 61-72, 2013.

MERZ, B.; HALL, J.; DISSE, M.; SCHUMANN, A. Fluvial flood risk management in a changing world. *Natural Hazards and Earth System Sciences* 10, 509–527, 2010.

MUNICH RE. Annual Review*:* Natural Catastrophes *2005*, Munich: *Munich Reinsurance Company*, 2005.

NAULIN, J.P.; PAYRASTRE, O.; GAUME, E. Spatially distributed flood forecasting in flash flood prone areas: Application to road network supervision in Southern France. *Journal of Hydrology*, v. 486, 88–99, 2013.

PETTA, R.; SINDERN, S.; CAMPOS, T. F. C.; NASCIMENTO, P. S. R. Integração e Análises Urbanas do Plano Diretor de Mossoró utilizando-se SIG e Sensoriamento Remoto. *In*: SIMPÓSIO BRASILEIRO DE SENSORIAMENTO REMOTO, 14, p. 795-802, 2009.

ROCHA, A. B. Proposta metodológica de gestão dos espaços-riscos de inundações urbana em Mossoró-RN. 2015. 172f. Tese (Doutorado em Geografia). Programa de Pós-Graduação em Geografia, Universidade Federal do Ceará, Fortaleza-CE, 2015.

SANTOS, W.O. Máximas intensidade e índices de Erosividade de chuvas para o Rio Grande do Norte. 2015. 142f. Tese (Doutorado em Manejo de Solo e Água). Programa de Pós-Graduação em Manejo de Solo e Água, Universidade Federal Rural do Semi-Árido, Mossoró-RN, 2015.

SATO, T. Fundamental characteristics of flood risk in Japan's Urban Areas. Society to Emerging Disaster Risks in Mega-Cities. Terra, p. 23-40, 2006. Disponível em: http://www.terrapub.co.jp/e-library/nied/pdf/023.pdf. 2006. Acesso em: 23/09/2020.

SILVA, A. A. Classificação orientada a objeto para mapeamento da cobertura vegetal da zona urbana de Mossoró/RN. 2015. 151f. Dissertação (Mestrado em Ciências Naturais). Programa de Pós-Graduação em Ciências Naturais, Universidade do Estado do Rio Grande do Norte, Natal-RN, 2015.

STERN, N. H. The economics of climate change: The Stern review. Cambridge, UK: Cambridge University Press, 2007.

TEHRANY, M.S.; PRADHAN, B.; JEBUR, M.N. Spatial prediction of flood susceptible areas using rule based decision tree (DT) and a novel ensemble bivariate and multivariate statistical models in GIS. *Journal of Hydrology*, v. 504, 69-79, 2013.

TELLMAN, B., SULLIVAN, J. A., KUHN, C., KETTNER, A. J., DOYLE, C. S., BRAKENRIDGE, G. R., Slayback, D. Satellite imaging reveals increased proportion of population exposed to floods. Nature, 596(7870), 80–86, 2021.

TUCCI, C.E.M.; PORTO, R.L.L.; BARROS, M.T. (org.). *Drenagem urbana*. Porto Alegre, ABRH, 1995. 384p.

UNDESA - UNITED NATIONS DEPARTMENT OF ECONOMIC AND SOCIAL AFFAIRS/POPULATION DIVISION. *World Urbanization Prospects: The 2011 Revision*. United Nations, New York. 2012

ZHANG J, CHEN Y. Risk assessment of flood disaster induced by typhoon rainstorms in Guangdong province, China. *Sustain*, v. 11, 2019.